Malaysian Journal of Analytical Sciences, Vol 22 No 6 (2018): 984 - 998
DOI: https://doi.org/10.17576/mjas-2018-2206-08

MALAYSIAN JOURNAL OF ANALYTICAL SCIENCES
Published by The Malaysian Analytical Sciences Society
ISSN 1394 - 2506

EFFECT OF GRAPHENE OXIDE AND CELLULOSE NANOFIBER TOWARDS MECHANICAL PROPERTIES OF POLYLACTIC ACID BASED ACTIVE PACKAGING USING RESPONSE SURFACE METHODOLOGY

(Kesan Grafin Oksida dan Gentian Fibril Selulosa Terhadap Kekuatan Mekanikal Pembungkus Aktif Menggunakan Kaedah Gerak Balas Permukaan)

Mohd Harfiz Salehudin[1] and Ida Idayu Muhamad [1,2]*

[1]*Bioprocess and Polymer Engineering Department, School of Chemical and Energy Engineering, Faculty of Engineering*
[2]*Cardiac Biomaterials Cluster, IJN-UTM Cardiovascular Engineering Center Level 2, Block B, Building V01, School of Biomedical Engineering, Faculty of Engineering*
Universiti Teknologi Malaysia, 81310 Johor Bahru, Johor, Malaysia

**Corresponding author: idaidayu@utm.my*

Received: 16 April 2017; Accepted: 18 November 2018

Abstract

A simple preparation of functional nanoscale graphene oxide (GO) *via* synthetic route was done using modified Hummer's Method whilst cellulose nanofiber from oil palm empty fruit bunch fiber was prepared using acid hydrolysis method. An active polylactide based nanocomposite film was prepared by incorporation of cellulose nanofiber (CNF), graphene oxide (GO) and essential oil (EO). In determining of factor influences the mechanical properties (tensile strength, elongation percentage and Young's modulus), the response surface methodology (RSM) Box Behnken Design (BBD) were used. The factors considered were the ratio (wt.%) of GO and CNF as an additive and 5 wt.% of EO was set as minimum. The mechanical properties that interpreted as tensile strength, percent elongation and Young's modulus were the response variables investigated. The ratio of EO wt.% (C) is found to be the most significant factor that influences the tensile strength of the nanocomposite. In the case of elongation percentage (%E) the percentage of cellulose nanofiber CNF (A) gave the most significant effect, where in Young's modulus, EO wt.% (C) is the most significant effect, followed by wt.% of GO (B). Validation of optimization by carrying out the confirmation run high degree of prognostic ability of response surface methodology. The results showed that the optimized formulation provided a mechanical strength (tensile strength, percentage elongation and Young's Modulus) pattern that is similar to the predicted curve, which indicated that the optimal formulation could be obtained using RSM.

Keywords: cellulose nanofiber, graphene oxide, mechanical properties, active packaging, essential oil

Abstrak

Penyediaan sintetik serphihan nano grafin oksida telah dilakukan melalui kaedah terubahsuai Hummer. Selulosa nanofiber dari tandan kelapa sawit telah disediakan dengan menggunakan kaedah hidrolisis asid. Filem komposit aktif nano polilaktik disediakan melalui penggabungan selulosa nanofiber, grafin oksida dan minyak pati. Dalam mengenal pasti faktor nisbah bahan penambah ke atas sifat-sifat mekanik, reka bentuk eksperimen yang sistematik berdasarkan kaedah gerak balas permukaan (RSM), rekabentuk Box-Behnken (BBD) telah digunakan. Faktor yang dikaji adalah nisbah (wt.%) daripada GO dan nanofibril selulosa (CNF) sebagai bahan tambahan dan minimum berat 5 wt.% sebagai berat minyak pati (EO) telah ditetapkan. Sifat-sifat mekanik yang terdiri daripada kekuatan tegangan, peratus pemanjangan dan modulus Young's adalah respon yang ditetapkan. Nisbah peratusan berat (wt.%) EO didapati menjadi faktor yang paling penting yang mempengaruhi kekuatan tegangan filem. Dalam kes peratusan pemanjangan (%E), CNF (A) didapati menjadi faktor utama yang mempegaruhi peratus pemanjangan, dimana dalam modulus Young's, EO wt.% (C) menjadi faktor utama dituruti peratus GO (B). Pengesahan pengoptimuman dijalankan untuk menguji tahap kemampuan respon prognostik keadah gerak balas permukaan. Hasil kajian menunjukkan

bahawa pengoptimaan untuk kekuatan mekanikal (kekuatan tegangan, peratus tegangan dan modulus Young's) menyerupai corak yang seperti diramalkan, menunjukkan bahawa pengoptimaan boleh didapati menggunakan RSM.

Kata kunci: gentian nanosellulosa, grafin oksida, sifat mekanikal, pembungkusan aktif, minyak pati

Introduction

In general, polylactic (PLA) biopolymers are naturally brittle and poorer mechanical properties than the conventional non-biodegradable plastic films used in the food packaging industries [1]. However, PLA a type of biopolymer can be designed and casted as thin film for various purpose by incorporation of different filler and additives. Polymer/nanofiber/nanosheet nanocomposites have significantly established attention compared to conventional composites because they often exhibit substantial improvement in term of physical, mechanical, barrier, thermal and optical properties [2]. Those improvements mentioned can be achieved by incorporating low filler or additives into the PLA based polymer as reported by previous studies; 0.1-1% cellulose nanofiber and 0.1-1 graphene oxide [3], 1-5 wt.% nanocellulose/nanoclay [2], 1%-10% cellulose nanowhiskers/ montromorillonite and others. In making PLA based active film for application in food packaging, an active compound need to be incorporated either by coating or applied directly into the packaging during film formation. The active compound in the packaging will then release to the food surrounding to kill pathogen/microbes hat responsible for food spoilage. The most natural and safer choice of antimicrobials is a volatile and phenolic compound that can be found in essential oil [4]. However, the addition of essential oil or oil-based antimicrobial into the polymer packaging decrease the tensile strength and Young's modulus [5]. It was found that the tensile strength of the film added with clove and thyme essential oil were lower than neat film. It was also reported that the results attributed by the breakup of film network that caused by essential oil addition [6-7].

The usages of cellulose nanofiber and graphene oxide on the other hand are quite new. Its potential in active packaging and controlled release are not fully explored. With the better insight of both nanomaterials in term of its functional properties, chemical and physical properties, the PLA film can be modified to serve specific purpose. As a result, the incorporation of cellulose nanofiber and graphene oxide into the bio plastic may enhance the physical characteristics of the film and able to control the release of active agents (such as pesticide and repellent). It is important in food packaging applications as well as food commodity and related sector. This finding may solve or at least reduce numerous species of insects and mites attack on the plant during the period of cultivation and also storage that known as a major reason of dreadful economic loss. Cellulose nanofiber, one form of nanomaterial has attracted massive attention because of its small size that interacts better with biodegradable polymer matrix. It is also more compatible when applied in flexible thin film. Cellulose nanofiber (CNF) could give excellent mechanical properties to the biodegradable plastic as it may exhibits comparable strength to petroleum-based plastic.

In its crystal region, cellulose nanofiber has high Young's modulus approximately at 138Gpa [8] also gives a very low coefficient of thermal expansion along longitudinal direction [9]. This expounds that nano-size cellulose has a big potential in the development of new and enhanced biopolymers. Graphene oxide is newly emerged nanomaterial with unique dimensional structure (one to two atom sheet) that might provide new functionality (controlled release of pesticide). Graphene sheet possesses numerous oxygen-containing groups on the surface, such as hydroxyls, epoxides, carbonyls, and carboxyls [10, 11]. These available oxygen containing group can facilitates the interaction between polymer hosts and graphene oxide, also between graphene oxide and active compound (repellant) via covalent or non-covalent bonds [11]. Hence, the addition of both nanomaterial serves different purpose. Cellulose nanofiber is found to be an approach to enhance the mechanical and physical properties of the PLA based packaging. The graphene oxide (GO) in PLA on the other hand may provide more efficient pesticide delivery hence reduce pesticide usage & adverse effect. In term of formulation and experimental design procedure, previous research on nanocomposite packaging involves the use of one-factor-at-a-time experimental approach. It is known as time consuming approach, cost higher, and also neglects the effect of interaction between factors.

Thus, this study attempts to investigate the percentage addition (wt.%) of nanofiller used on the mechanical characteristics of active nanocomposite film using response surface method (RSM). The RSM enables the prediction of the optimum composition of CNF, GO and EO to the production PLA nanocomposite film. This study covered the effect of GO, CNF and EO towards the mechanical properties of the active film formed. The statistical

analysis using respond surface methodology was used to compute the optimal additive (CNF/GO/EO) to be added into an active film to provide the optimum mechanical properties.

Materials and Methods

Materials

Oil palm empty fruit bunch (OPEFB) fiber was retrieved from Universiti Kebangsaan Malaysia - Malaysia Palm Oil Board (UKM-MPOB) research center, Bangi, Malaysia. Sulfuric acid (Sigma Aldrich®), graphite fine powder (VChem ®), sodium nitrate (Qrec), hydrogen peroxide (GCE) were used to synthesize graphene oxide. Polylactic acid (Natureworks), chloroform (Fischer Scientific), and thyme essential oil (Sigma-Aldrich) were used as based film.

Nanomaterials preparation and characterization

Cellulose nanofiber (CNF) from oil palm empty fruit bunch (OPEFB) was prepared and characterized as described in previous method [12]. Graphene oxide nanosheet was synthesized *via* modified Hummer's method. Physical and chemical characterization of graphene nanosheet was done through field emission scanning electron microscope (FESEM) with energy dispersive X-ray spectroscopy (EDX), Fourier transform infrared spectroscopy (FTIR), and Fourier Atomic-Force Microscopy (AFM).

Polylactic acid based active nanocomposite film

In nanocomposite film making, CNF and GO were dispersed in chloroform to known concentration, the same solvent that used to dissolve PLA in this experiment. The dispersion takes place *via* solvent exchange, where the graphene oxide and cellulose nanofiber was first dispersed into acetone then into chloroform. Next, PLA pellet, CNF, GO and EO was dispersed in chloroform at temperature 60 ◦C in water bath for two hours. The mixture was cast on 19cm x 10cm acrylic plate and dried at room temperature overnight. The formed film was conditioned in desiccator for 48 hours.

Mechanical strength evaluation

Referring to method ASTM D 882-02, the mechanical strength Young modulus (Y) tensile strength (TS), and percentage elongation (%E) of prepared nanocomposite was evaluated using texture analyzer CT3 (Brookfield, USA). TA-DGA fixture accessories for packaging and thin sheet polymer was specifically used. The gauge length was set to 5 cm with crosshead speed 0.5 mm/min. In sampling preparation, films were cut into rectangular shape (8cm x 1cm). Total average of five specimens will be recorded for each test. The purpose of this test is to investigate the effect of cellulose nanofiber and graphene oxide incorporation percentage to the mechanical strength of the film that is being formed.

Experimental design

The response surface design is developed based on three factors, three level Box-Behnken. The design consists of a replicated center point and a set of points lying at the midpoint of each edge of the multidimensional cube that defines the region of interest. The processing material, independent and dependent variables involved in the design are listed in Table 1. The experimental design generated using the Design Expert Version 6.0 software. The 3-D response surface plots were also drawn using this software. The design involved 17 runs with five replications and the response variables measured were the tensile strength and elongation percentage (%E) as shown in Table 2. The nonlinear, quadratic model is given as:

$$Y = b0 + b1(CNF) + b2(GO) + b3(EO) + b12(CNF)(GO) + b13(CNF)(EO) + b23(GOEO) + b11(CNF)^2 + b22(GO)^2 + b33(EO)^2 \quad (1)$$

where y is the measured response associated with each factor level combination; b0 is an intercept; b1 to b33 are regression coefficients computed from the observed experimental values of Y; and CNF, GO and EO are the coded levels of independent variables and E is the error term. The statistical validity of the polynomials was established on the basis of ANOVA provision in the Design Expert Software. Finally, the feasibility and grid searches were performed to locate the composition of optimum formulations.

Table 1. Variables in Box-Behnken design

Factor	Levels		
	Low	Medium	High
CNF = Cellulose Nanofiber	0	0.75	1.5
GO = Graphene Oxide	0	0.75	1.5
EO = Essential oil	5	10	15

Table 2. Design layout and experimental results for Box-Behnken design

Run	Independent Factor			Response		
	X1	X2	X3	Y1 (Tensile)	Y2 (%E)	Y3 (YM)
1	0.75	1.50	15.00	12.48	134.27	6.76
2	0.00	0.75	5.00	20.69	235.93	9.544
3	0.75	0.75	10.00	14.38	210.22	8.642
4	0.00	1.50	10.00	15.36	179.16	7.406
5	0.75	1.50	5.00	26.38	45.16	6.144
6	1.50	1.50	10.00	26.50	7.84	7.711
7	1.50	0.75	5.00	37.90	2.93	8.187
8	0.75	0.75	10.00	12.54	247.95	9.898
9	0.75	0.75	10.00	14.27	211.63	9.07
10	0.00	0.75	15.00	12.41	130.34	2.891
11	1.50	0.00	10.00	23.27	7.78	4.719
12	0.75	0.00	5.00	22.39	3.22	6.971
13	0.75	0.00	15.00	9.44	108.31	1.587
14	1.50	0.75	15.00	16.38	11.10	4.623
15	0.75	0.75	10.00	13.23	231.96	9.738
16	0.00	0.00	10.00	20.62	4.15	2.459
17	0.75	0.75	10.00	13.52	222.86	9.102

All check points performed over the entire experimental domain to validate the chosen experimental design and polynomial equations. The formulations corresponding to these check points were prepared and evaluated for various response properties

Results and Discussion

The neat PLA based film was prepared without the addition of CNF, GO and EO was evaluated for its mechanical properties. The tensile strength, elongation percentage, and Young's modulus of neat PLA based packaging obtained was 18.51 ± 0.2 MPa, 87.54 ± 0.1%, and 4.5 GPa that is on par with the result obtained by Arjmandi et al. [13] and Chen et al. [3]. Both researchers stated that the tensile and Young's modulus were at range 17-20 Mpa, and 3-4.5 GPa, respectively. The nanocomposite packaging produced was evaluated and per experimental plan are shown in Table 2. The tensile strength, elongation percentage (%E), and Young's modulus results were input into the Design Expert software for further analysis. Examination of the fit summary output revealed that the quadratic model is statistically significant for the tensile, elongation percentage and Young's modulus. Therefore, both these models for tensile and elongation were used to represent each of the responses for further analysis.

ANOVA analysis

For the response surface methodology based on Box – Behnken design, 17 experiments were required. The experimental runs and the observed responses for the 17 formulations are given in Table 2. In evaluation of a good optimization model, test for significance of regression model, test for significance on individual model coefficients and test for lack-of-fit need to be performed. An ANOVA table is commonly used in summarized the tests performed. In general, at 5% level of significance, a model is considered statistically significant if the p – value is less than 0.05. The ANOVA analysis for the response surface, quadratic model for tensile strength is shown in Table 3.

Table 3. ANOVA table (sum of square) for quadratic model (Response: Tensile strength)

Source	Sum of Square	DF	Mean Square	F	Prob > F	
Block	37.73	2	18.86			
Model	790.85	9	87.87	32.94	0.0006	significant
A	152.86	1	152.86	57.31	0.0006	
B	5.96	1	5.96	2.23	0.1953	
C	399.4	1	399.4	149.74	< 0.0001	
A2	151.23	1	151.23	56.7	0.0007	
B2	0.42	1	0.42	0.16	0.7068	
C2	14.82	1	14.82	5.56	0.065	
AB	24.42	1	24.42	9.15	0.0292	
AC	50.98	1	50.98	19.11	0.0072	
BC	0.23	1	0.23	0.085	0.7829	
Residual	13.34	5	2.67			
Lack of Fit	11.61	3	3.87	4.48	0.1879	not significant
Pure Error	1.73	2	0.86			
Cor Total	841.92	16				
Standard Deviation	1.73					
Mean	18.34		R^2 =	0.9834		
			Adjusted R^2 =	0.9536		
			Predicted R^2 =	N/A		
			Adequate precision =	19.839		

In Table 3, the values of "prob>F" for the model is less than 0.05; which indicates that the model is significant. It is desired as it indicates that the model has a significant effect on the response. In a similar manner, the main effect of essential oil EO (C), cellulose nanofiber CNF (A), and the quadratic interaction of CNF (A) with EO (C) designated as (AC) and CNF (A) with graphene oxide (GO) designated by (AB) are significant model terms. Other model terms can be classified as insignificant. An improved model otherwise, can be developed by eliminating the insignificant model. The lack-of-fit in the model shows as insignificant. Insignificant model term in lack-of-fit is desirable as we want a model that fits. The regressive elimination procedure was performed to automatically reduce the insignificant terms. As a result, the ANOVA table for the reduced quadratic model is tabulated in Table 4. The results designated that the model remains significant. The significant model terms are still the same as mentioned in Table 3. The significant factors were ranked based on the value of F-ratio. The larger the magnitude of F-value and correspondingly the smaller the "prob>F" value, the more significant is the corresponding coefficient [14, 15].

Thus, in this study, the ranking is as follows**:** C> A> AC> AB> B. The R-squared (R^2)-value calculated is 0.98. The value is close to 1 which is reasonably acceptable. that close to 1. It signifies that about 98.3% of the variability in the data is explained by the model. Adequate precision on the other hand compares the range of the predicted values at the design points to the average prediction error. Ratios greater than 4 indicate adequate model discrimination. In this case, the value is well above 4. The exact same method is also applied to the other response, percentage elongation (%E) and Young's modulus. The ANOVA analysis of the quadratic model of elongation (%E) and Young's modulus was tabulated in Table 5 and Table 6, respectively. In response variable on of elongation percentage (%E), it's shown that cellulose nanofiber (CNF), second order of effect of cellulose nanofiber CNF (A^2), and effect of ratio CNF to GO (AB) are the significant model terms. The R^2 value for percentage elongation is 0.92486 that adjacent to 1 which shows the desirable characteristic for a good model. The ANOVA for Young's modulus as shown in Table 6, indicates that the model is significant as the "prob>F" is less than 0.05. It also indicates that the terms in the model have a significant effect on the response. In Young's modulus the ranking of significant factor that affecting Young's modulus is as follows; C> B> A^2> BC> C^2> B^2> AC. The other model on the other hand are said to be not significant.

Table 4. ANOVA table for reduced quadratic model (response: Tensile strength)

Source	**Sum of Squares**	**DF**	**Mean Square**	**F Value**	**Prob > F**	
Block	37.73	2	18.86			
Model	790.63	8	98.83	43.72	< 0.0001	significant
A	152.86	1	152.86	67.63	0.0002	
B	5.96	1	5.96	2.63	0.1557	
C	399.40	1	399.40	176.70	< 0.0001	
A2	151.23	1	151.23	66.90	0.0002	
B2	0.42	1	0.42	0.19	0.6803	
C2	14.82	1	14.82	6.56	0.0429	
AB	24.42	1	24.42	10.80	0.0167	
AC	50.98	1	50.98	22.55	0.0032	
Residual	13.56	6	2.26			
Lack of Fit	11.83	4	2.96	3.42	0.2386	not significant
Pure Error	1.73	2	0.86			
Cor Total	841.92	16				
Std. Deviation	1.50					
Mean	18.34		R^2 =	0.98		
			Adjusted R^2 =	0.96		
			Predicted R^2 =	N/A		
			Adequate precision =	22.71		

Table 5. ANOVA table (sum of square) for quadratic model (Response: Percentage elongation)

Source	Sum of Square	DF	Mean Square	F	Prob > F	
Block	33475.71	2	16737.85			
Model	1.14E+05	9	12661.41	6.84	0.0238	significant
A	33790.9	1	33790.9	18.25	0.0079	
B	3325.7	1	3325.7	1.8	0.2379	
C	3333.73	1	3333.73	1.8	0.2374	
A^2	28292.38	1	28292.38	15.28	0.0113	
B^2	5560.15	1	5560.15	3	0.1437	
C^2	7614.1	1	7614.1	4.11	0.0984	
AB	13195.11	1	13195.11	7.13	0.0444	
AC	7489.95	1	7489.95	4.05	0.1005	
BC	63.84	1	63.84	0.034	0.86	
Residual	9258.06	5	1851.61			
Lack of Fit	8540.77	3	2846.92	7.94	0.1139	not significant
Pure Error	717.29	2	358.64			
Cor Total	1.57E+05	16				
Standard Deviation	43.03					
Mean	117.34		R^2 =	0.92		
			Adjusted R^2 =	0.79		
			Predicted R^2 =	N/A		
			Adequate precision =	7.28		

Table 6. ANOVA table (sum of square) for quadratic model (Response: Young's modulus)

Source	Sum of Square	DF	Mean Square	F	Prob > F	
Block	31.49	2	15.75			
Model	77.63	9	8.63	9.73	0.0110	significant
A	1.08	1	1.08	1.22	0.3199	
B	13.93	1	13.93	15.71	0.0107	
C	21.62	1	21.62	24.38	0.0043	
A^2	9.48	1	9.48	10.69	0.0222	
B^2	4.67	1	4.67	5.27	0.0702	
C^2	8.13	1	8.13	9.17	0.0292	
AB	2.27	1	2.27	2.56	0.1708	
AC	4.12	1	4.12	4.65	0.0836	
BC	9.00	1	9.00	10.15	0.0244	
Residual	4.43	5	0.89			

Table 6 (cont'd). ANOVA table (sum of square) for quadratic model (Response: Young's modulus)

Source	Sum of Square	DF	Mean Square	F	Prob > F	
Lack of Fit	3.50	3	1.17	2.49	0.2990	not significant
Pure Error	0.93	2	0.47			
Cor Total	113.55	16				
Standard Deviation	0.94					
Mean	6.79		R^2 =	0.95		
			Adjusted R^2 =	0.85		
			Predicted R^2 =	N/A		
			Adequate precision =	11.25		

The final empirical models in terms of coded factors were presented as follows (equation 2-4):

$$Y^1(\text{Tensile}) = 13.94 + 4.37A + 0.90B - 7.35C + 6.28A^2 + 0.46B^2 + 1.96C^2 + 2.67AB - 3.86AC - 0.24BC \quad (2)$$

$$Y^2(\%\ \text{Elongation}) = 212.38 - 64.99A + 21.22B + 21.25C - 85.84A^2 - 53.27B^2 - 44.53C^2 - 62.04AB + 46.74AC - 3.99BC \quad (3)$$

$$Y^3(\text{Young's Modulus}) = 9.04 + 0.37A + 1.37B - 1.71C - 1.57A^2 - 1.54B^2 - 1.45C^2 - 0.81AB - 1.10AC + 1.50BC \quad (4)$$

In actual factor terminology, the final experimental models are presented as equation 5-7:

$$Y^1(\text{Tensile}) = 32.45976 - 4.18167CNF - 2.96708GO - 2.22373EO + 11.15648CNF^2 + 0.82648GO^2 + 0.078579EO^2 - 4.74407(CNF)(GO) - 1.02828(CNF)(EO) - 0.063333(GO)(EO) \quad (5)$$

$$Y^2(\%\ \text{Elongation}) = -80.12 + 100.32CNF + 263.73GO + 31.32EO - 152.60CNF^2 - 94.71GO^2 - 1.78EO^2 - 110.29(CNF)(GO) + 12.46(CNF)(EO) - 1.07(GO)(EO) \quad (6)$$

$$Y^3(\text{Young's Modulus}) = 6.16877 + 2.83900CNF + 3.03308GO + 0.30246EO - 2.79256CNF^2 - 2.74522GO^2 - 0.058198EO^2 - 1.44511(CNF)(EO) - 0.29237(CNF)(EO) + 0.4(GO)(EO) \quad (7)$$

Within the limits of the experiment, the tensile strength, percentage elongation and Young's modulus can be predicting by using this model. Figures 1 (a-f) shown the normal probability plot of the residuals and the plot of the residuals versus the predicted response for tensile strength, percentage elongation and Young's modulus.

Plot pattern on the Figures 1 (a, c, e) revealed that the residuals mostly fall on a straight line inferring that errors are distributed normally, and thus, support adequacy of the least-square fit [16]. Figures 1 (b, d, and f) presented that they have no obvious pattern and unusual structure. The point also scattered equally above and below the x-axis. This suggests that the models proposed are satisfactory and there is no reason to suspect any violation of the independence or constant variance assumption.

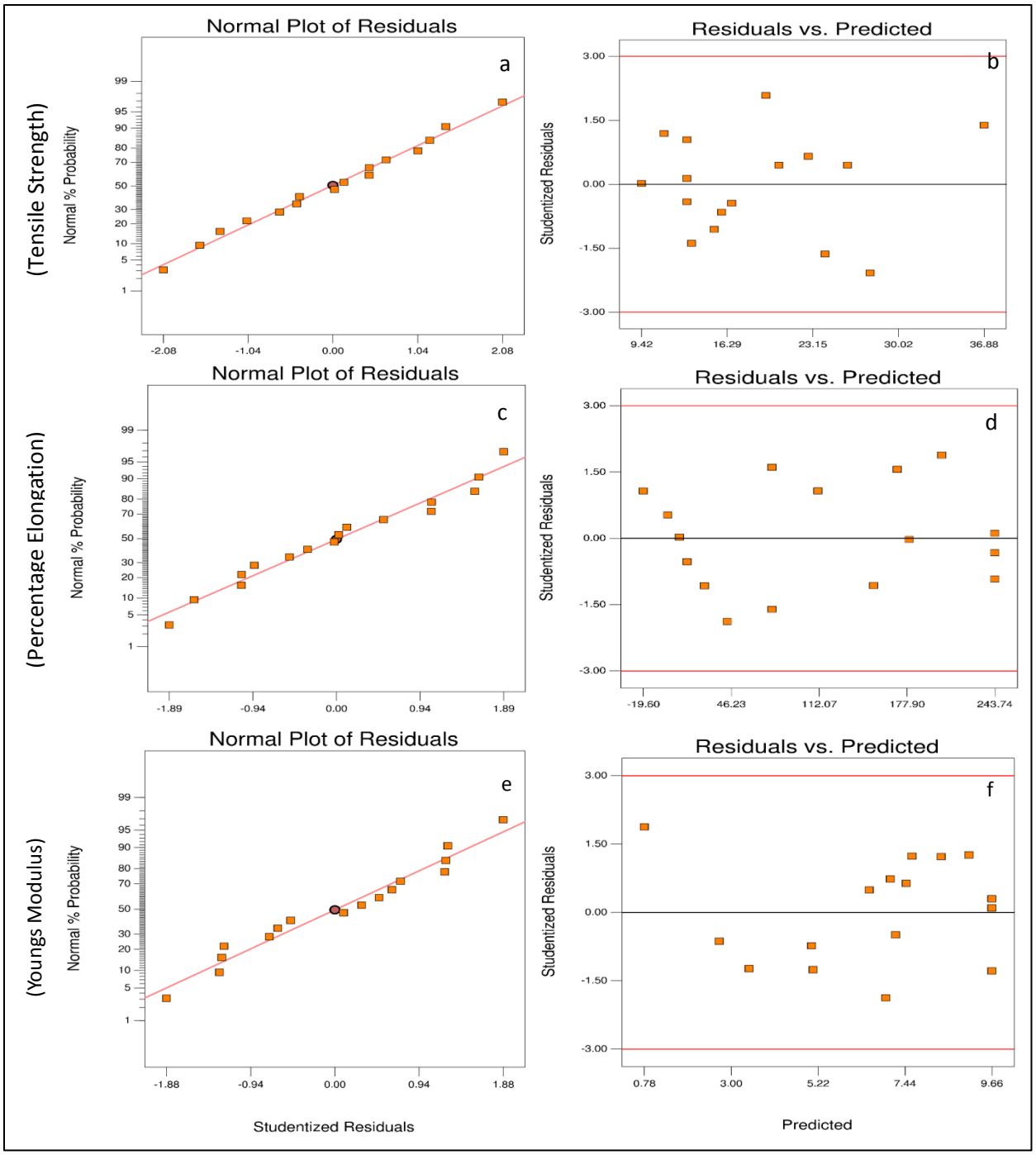

Figure 1. Normal probability plot of residual for tensile strength (a), percentage elongation (c), and Young's modulus (e) respectively, and plot of residual *vs* predicted response for strength (b), percentage elongation (d), and Young's modulus (f)

Effect of factor variables on tensile, elongation and Young's modulus

The effect of different factor variables on tensile strength, percentage elongation and Young's modulus are demonstrated by three-dimensional surface, and contour plate as depicted in Figure 2, 3 and 4, respectively. The 3D surface graph for the tensile strength has a hyperbolic profile in accordance to the quadratic model and is shown in Figure 2(a). The contour plot for the response surface for tensile strength is shown in Figure 2(b). In a condition where the essential oil is keeping at the middle level (10), the effect of the ratio of CNF (A) and GO (B) can be clearly seen in Figure 2(a). At the lowest level of CNF and GO, the tensile was 18.08 MPa. The increase and decrease of tensile strength are dependent on amount of GO and CNF. The maximum tensile strength was determined at 38.0617 Mpa when the ratio of CNF was at 1.5% and G.O at 0.82 as interpreted by numerical optimization on Figure 2(c).

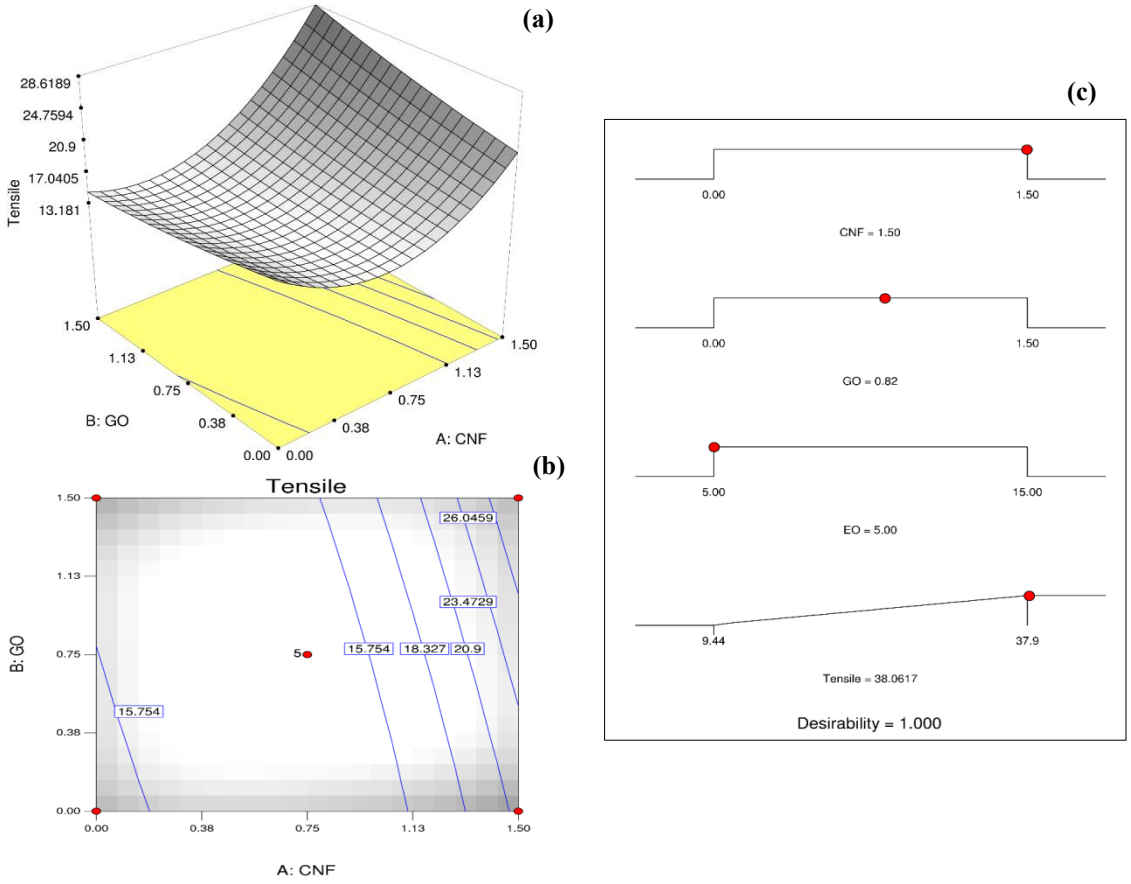

Figure 2. Surface (a) and contour (b) plot on tensile of CNF and GO (c) numerical optimization

The surface and contour plots of the ratio of CNF versus GO on the percentage elongation are presented in Figure 3. At fixed GO and EO concentration, the elongation increased with the increase of CNF ratio that is until 0.59% then decreased with the increase of CNF in the rest of region. Similar pattern shown when the EO and CNF were kept at minimum of addition percentage. The elongation increased with the increment of GO ratio until 0.89% addition and the elongation was decreased in the rest of the region. Numerical optimization of the elongation percentage was depicted in Figure 3(c). The effect of factor CNF and GO on the response Young's modulus represented in Figure 4. From the 3D surface diagram (Figure 4a), the maximum Young's modulus 9.62 GPa can be achieved when the amount of CNF and GO were at 0.66% and 0.92%, respectively. Any addition of CNF and GO after that point, can cause the decrement of Young's modulus.

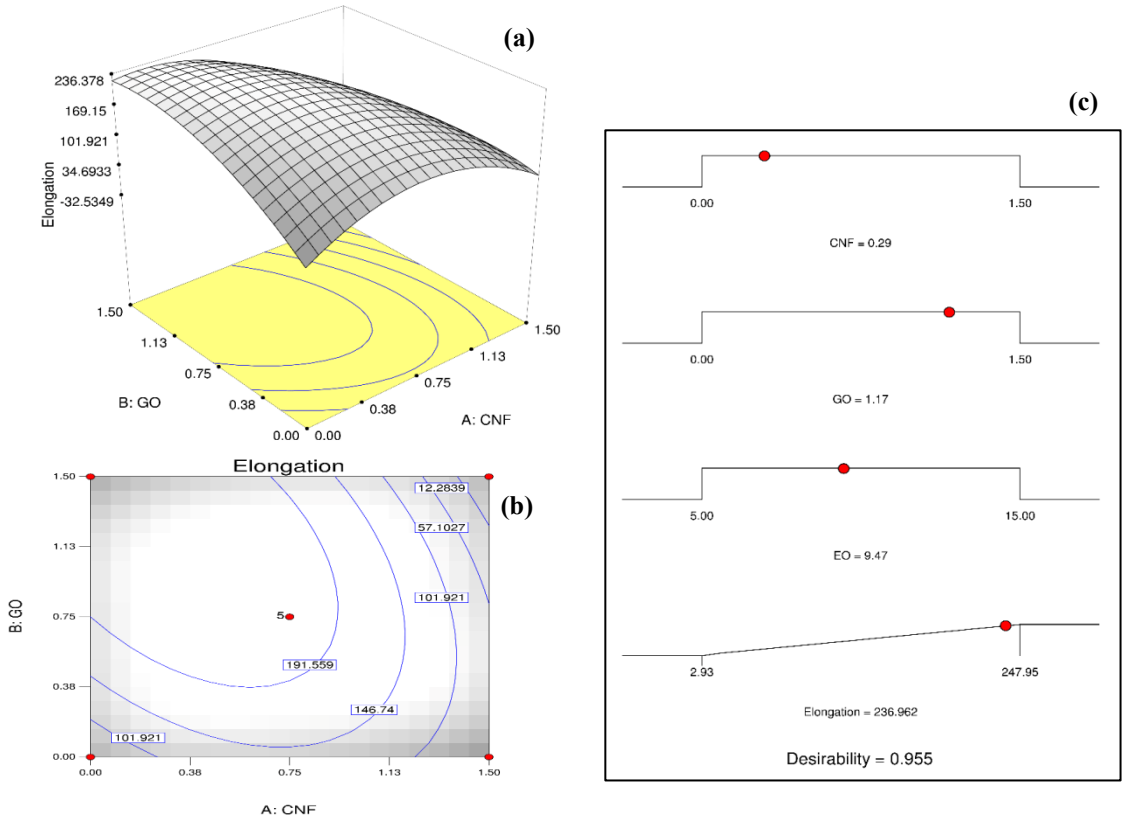

Figure 3. Surface (a) and contour (b) plot on percentage elongation of CNF and GO (c) numerical optimization

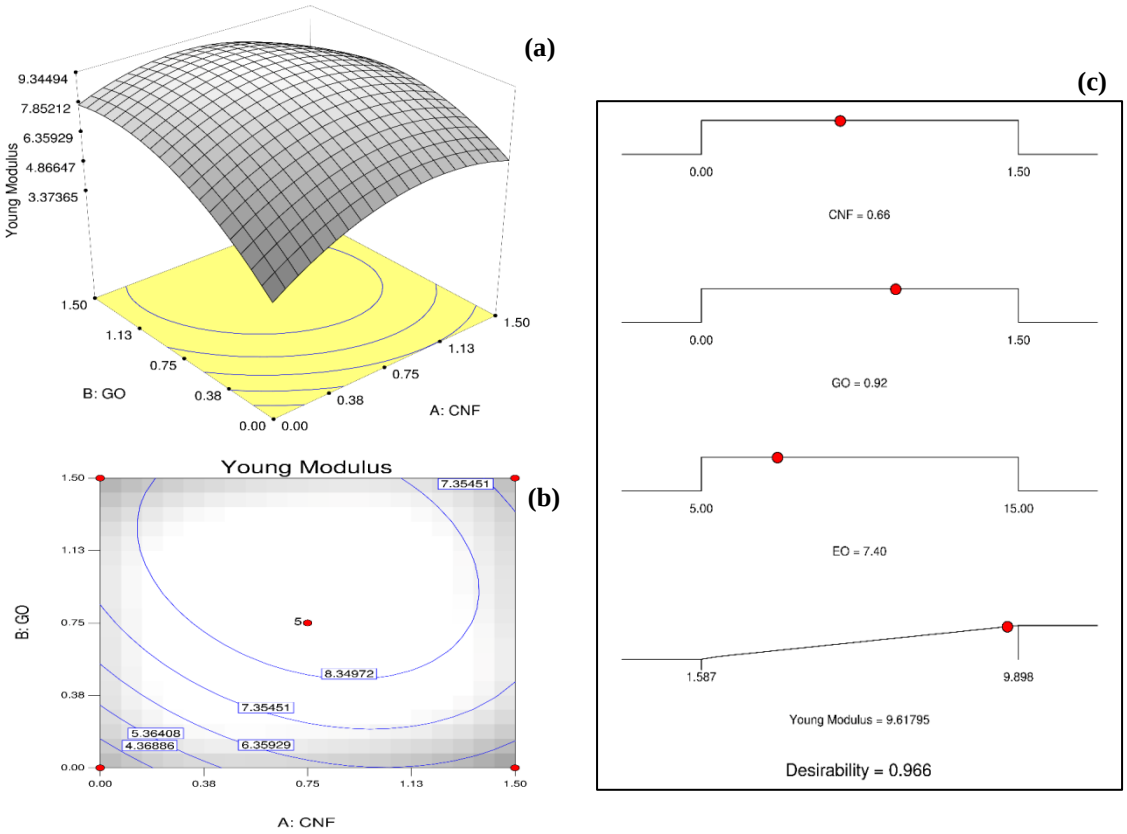

Figure 4. Surface (a) and contour (b) plot on Young's modulus of CNF and GO (c) numerical optimization

From the results obtained, it shows that increment of percentage additives (CNF, GO and EO) positively affects the mechanical properties (tensile strength, elongation percentage and Young's Modulus) until a certain point that lies within the limits of the factors being investigated. Typically with many nanocomposite systems, adding 1% and 2% by weight of graphene oxide showed slightly decreased mechanical properties due to aggregation of graphene oxide at this point [17]. Similar pattern was reported by Ionita et al. who found that the modulus and tensile strength increased at low concentration of graphene oxide but the mechanical properties decreased when the GO reached 2 wt.% [18]. These studies lead to the conclusion that generally GO has poor dispersion at high loading in most polymer matrices hence reduce the mechanical properties. The addition of CNF and EO also exhibits the same pattern that shows improvement on mechanical properties with the addition of low filler concentration that varied between 0-1 wt.% [19]. The effect of both nanofiller addition in packaging polymer towards the mechanical properties are not widely studied. However, this RSM study can be used to primarily visualizing or predict the behavior of the mechanical properties. It gives an insight to researcher to identify the significant effect of the addition of nanofiller percentage (wt.%) in this research and provides a framework for further investigation.

Confirmation run

Eight random check point formulations for which the results of all the dependent variables were found to be within the limits. Using experimental data, regression equations can be obtained in order to predict the tensile strength percentage elongation and Young's modulus at any particular ratio of CNF, GO and EO that lie in the limits tested. The predicted values and the actual experimental values were compared, the residual and the percentage error calculated. Table 7 lists the actual and predicted values of the check formulations among with the % prediction error in order to validate the model adequacy.

Table 7. Actual experimental value, predicted value, and error percentage of tensile, percentage elongation, and Young's modulus

Ratio of CNF, GO and EO			Tensile			Elongation			Young's Modulus		
CNF	**GO**	**EO**	**Actual Value**	**Predicted Value**	**Error**	**Actual Value**	**Predicted Value**	**Error**	**Actual Value**	**Predicted Value**	**Error**
0	0	10	20.62	19.38	1.24	4.15	13.17	-9.02	2.46	2.7	-0.24
1.5	0	10	23.27	22.79	0.48	7.78	7.26	0.52	4.72	5.06	-0.34
0	1.5	10	15.36	15.84	-0.48	179.16	179.68	-0.52	7.41	7.07	0.34
1.5	1.5	10	26.5	27.74	-1.24	7.84	-1.18	9.02	7.71	7.47	0.24
1.5	0.75	5	37.9	36.88	1.02	2.93	-19.60	22.53	8.19	7.62	0.57
0.75	1.5	15	12.48	10.98	1.50	134.27	111.21	23.06	6.76	6.53	0.23
0.75	0.75	10	13.52	13.52	0.00	222.86	222.86	0.00	9.1	9.1	0
0.75	0.75	10	12.54	13.06	-0.52	247.95	243.74	4.21	9.9	9.66	0.24

Correlation plot of linearity between the actual (experimental) value and predicted values are shown in Figure 5 (a), (b), and (c). The correlation obtained exhibits high R^2 values, 0.988, 0.9891, 0.9711 for tensile, percentage elongation, and Young's Modulus respectively. Thus, it can be said that the empirical models developed were reasonably accurate, for tensile, elongation % and young's modulus as all actual values for the confirmation runs are within the 95% prediction interval.

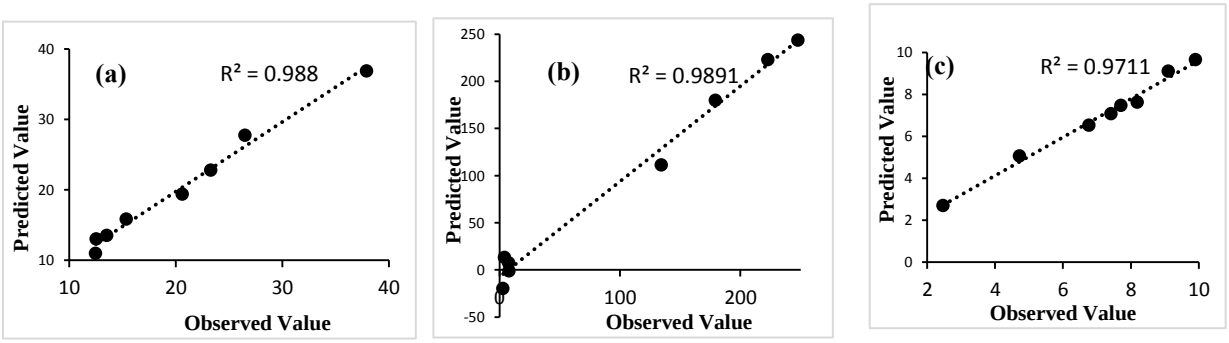

Figure 5. Linear correlation of predicted value *vs* observed value for (a) tensile strength (b) percentage elongation, and (c) Young's modulus

Multiple responses optimization

In packaging field, it is desirable if the packaging material exhibits certain mechanical characteristic by means high tensile strength, high percentage elongation (elasticity) and high Young's modulus. Multiple responses using the desirability approach is a procedure involves the optimization of more than one response. Once the optimization comprises multiple response (more than one), it is impossible to optimize each one separately because number of solutions equal to the variables under study, which are the amount of CNF, GO and EO would be gathered. The optimum level of the response variables was determined by desirability with the scale 0 to 1.0. As stated by Derringer and Suich [20], different desirability functions can be used, depending on the partial response that is required to be maximized, minimized or assigned target value. In this study, all the partial response, tensile, percentage elongation and Young's modulus were maximized. The factors (CNF, GO and EO % ratio) were set to within the range of limit of factors to be studied. Finally, one compromise solution was found for this multiple optimization and numerical ramp solution is shown in Figure 6. It shown the maximum response for tensile strength, percentage elongation and Young's modulus were interpolated to 21.39 Mpa, 182.68 % and 9.26 GPa,

respectively. The overall desirability on the other hand was calculated as the geometric average of the partial desirability functions of individual components. The overall desirability for this solution is 0.652. It shows that all responses are predicted to be within the desired limits. The possible solution was stated in the figure where CNF, GO and EO needed to be at the ratio of 0.51:0.99:5.00 weight percent respectively in order to reach maximum response.

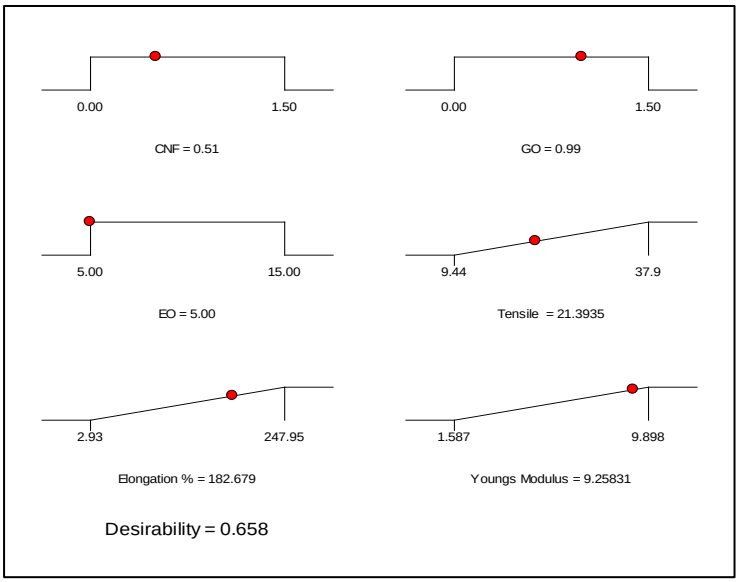

Figure 6. Multiple response using numerical ramp and desirability

Conclusion

The mechanical performance in term of tensile strength, percentage elongation (%E) and Young's modulus were analyzed using RSM method. The results from the analysis of variance (ANOVA) revealed that essential oil (EO) is the most significant factor that influences the tensile strength and it's followed by CNF (A), second order of CNF (A^2), interaction of CNF to EO (AC), and then followed by interaction of CNF to GO (AB). In the case of elongation percentage (%E), CNF (A) gave the most significant effect followed by second order effect of CNF (A^2), and then followed by the interaction of CNF to GO (AB). In Young's modulus, wt.% of EO (C) give the most significant effect followed by wt.% of GO (B). The ranking for the Young's modulus is as follows C> B> A^2> BC> C^2> B^2> AC. The multiple optimization for three responses; tensile, percentage elongation and Young's Modulus that were set to maximum yield one possible solution. The maximum tensile, elongation percentage and Young's modulus can be optimized up to 21.39 MPa, 182.68%, and 9.26 GPa, respectively that can be achieved by keeping the ratio of CNF, GO and GO at 0.51:0.99:5.00 (%), respectively. Overall, the validation of optimization technique demonstrated the reliability of the model. The experimental values of the response variables obtained from the optimized formulations were closed and in linear with the predicted values. Thus, the models developed using RSM were reasonably accurate and enabled the formulation of active packaging with desirable mechanical strength. The use of RSM approach also enable to identify the significant factor (the percentage of additives; CNF, GO, and EO) that affects the mechanical properties (tensile strength, elongation percentage and Young's Modulus). It was concluded that the appropriate statistical design and optimization techniques can be successfully used in the development of active packaging with predictable mechanical properties. The use of RSM approach enables the identification of significant factors for the wt.% of nanofiller addition in this research and finally provides a framework for further investigation.

Acknowledgement

The authors would like to thank Universiti Teknologi Malaysia (UTM), Ministry of Higher Education (MOHE), and Research Management Centre (RMC), UTM for their financial support of this work through the project number Q.J130000.7846.4F726.

References

1. Abdul Khalil, H. P. S., Bhat, I. U. H., Jawaid, M., Zaidon, A., Hermawan, D. and Hadi, Y. S. (2012). Bamboo fibre reinforced biocomposites: A review. *Materials and Design,* 42: 353-368.
2. Trifol, J., Plackett, D., Sillard, C., Szabo, P., Bras, J. and Daugaard, A. E. (2016). Hybrid poly(lactic acid)/nanocellulose/nanoclay composites with synergistically enhanced barrier properties and improved thermomechanical resistance. *Polymer International,* 65(8): 988-995.
3. Chan, C. H., Chia, C. H., Zakaria, S., Ahmad, I., Dufresne, A. and Tshai, K. Y. (2014). Low filler content cellulose nanocrystal and graphene oxide reinforced polylactic acid film composites. *Polymers Research Journal,* 9(1): 165-176.
4. Del Nobile, M. A., Lucera, A., Costa, C. and Conte, A. (2012). Food applications of natural antimicrobial compounds. *Frontiers in Microbiology,* 3(287): 1-13.
5. Silverajah, V. S., Ibrahim, N. A., Zainuddin, N., Yunus, W. M. and Hassan, H. A. (2012). Mechanical, thermal and morphological properties of poly(lactic acid)/epoxidized palm olein blend. *Molecules,* 17 (10): 11729-47.
6. Hosseini, M. H., Razavi, S. H. and Mousavi, M. A. (2009). Antimicrobial, physical and mechanical properties of chitosan-based films incorporated with thyme, clove and cinnamon essential oils. *Journal of Food Processing and Preservation,* 33: 727-743.
7. Pranoto, Y., Rakshit, S. K. and Salokhe, V. M. (2005). Enhancing antimicrobial activity of chitosan films by incorporating garlic oil, potassium sorbate and nisin. *Lebensmittel-Wissenschaft and Technologie,* 38(8): 859-865.
8. Sakurada, I., Nukushina, Y. and Ito, T. (1962). Experimental determination of the elastic modulus of crystalline regions in oriented polymers. *Journal of Polymer Science,* 57(165): 651-660.
9. Nishino, T., Matsuda, I. and Hirao, K. (2004). All-cellulose composite. *Macromolecules,* 37(29): 7683-7687.
10. Chen, J., Yao, B., Li, C. and Shi, G. (2013). An improved Hummers method for eco-friendly synthesis of graphene oxide. *Carbon,* 64: 225-229.
11. Tao, C. A., Wang, J., Qin, S., Lv, Y., Long, Y., Zhu, H. and Jiang, Z. (2012). Fabrication of pH-sensitive graphene oxide–drug supramolecular hydrogels as controlled release systems. *Journal of Materials Chemistry,* 22(47): 24856-24861.
12. Salehudin, M. H., Salleh, E., Muhamad, I. I. and Mamat, S. N. H. (2014). Starch-based biofilm reinforced with empty fruit bunch cellulose nanofibre. *Materials Research Innovations,* 18(S6): 322- 325.
13. Arjmandi, R., Hassan, A., Eichhorn, S., Mohamad Haafiz, M. K., Zakaria, Z. and Tanjung, F. (2015). Enhanced ductility and tensile properties of hybrid montmorillonite/cellulose nanowhiskers reinforced polylactic acid nanocomposites. *Journal of Materials Science,* 50(8): 3118-3130.
14. Cochran, W. G. and Cox, G. M. (1992). Experimental Designs, 2nd Edition. John Wiley & Sons, Inc, Canada.
15. Myers, R. H., Montgomery, D. C. and Anderson-Cook, C. M. (2009) Response surface methodology: Process and product optimization using designed experiments. Wiley, Hoboken, New Jersey.
16. Idris, A., Kormin, F. and Noordin, M. (2006). Application of response surface methodology in describing the performance of thin film composite membrane. *Separation and Purification Technology,* 49(3): 271-280.
17. Ammar, A., Al-Enizi, A. M., AlMaadeed, M. A. and Karim, A. (2016). Influence of graphene oxide on mechanical, morphological, barrier, and electrical properties of polymer membranes. *Arabian Journal of Chemistry,* 9(2): 274-286.
18. Ionita, M., Pandele, A. M., Crica, L. and Pilan, L. (2014). Improving the thermal and mechanical properties of polysulfone by incorporation of graphene oxide. *Composites Part B: Engineering,* 59: 133-139.
19. Lavoine, N., Desloges, I., Dufresne, A., Bras, J. (2012). Microfibrillated cellulose - its barrier properties and applications in cellulosic materials: A review. *Carbohydrate Polymer,* 90(2): 735-64.
20. Derringer, G. and Suich, R. (1980). Simultaneous optimization of several response variables. *Journal of Quality Technology,* 12: 214-219.